J|A|C|S COMMUNICATIONS

Published on Web 05/19/2010

Size-Selective Separation of Macromolecules by Nanochannel Titania Membrane with Self-Cleaning (Declogging) Ability

Poulomi Roy,[†] Tuli Dey,[†,‡] Kiyoung Lee,[†] Doohun Kim,[†] Ben Fabry,[‡] and Patrik Schmuki*[,†]

Department of Materials Science, WW4-LKO, University of Erlangen-Nuremberg, Martensstrasse 7, 91058 Erlangen, Germany and Center for Medical Physics and Technology, Department of Physics, University of Erlangen-Nuremberg, Henkestrasse 91, 91052 Erlangen, Germany

Received April 6, 2010; E-mail: schmuki@ww.uni-erlangen.de

Size selective separation of biologically relevant macromolecules using nanoporous channel membranes has for several years been a tempting topic in nanoengineering, chemistry, and medicine, as it allows for simple and direct purification of biomolecules such as proteins, as well as the mimicking biological membranes.[1−5]

The efficiency of size-dependent separation is determined by the relation of pore size to the effective hydrodynamic diameter (or the Debye radius, respectively) of the targeted molecules in a given electrolyte. Small protein molecules were reported to pass through porous channels with approximately three times their diameter,[4] though some unknown factors such as the physical shape of the protein, its 3-D hydrodynamic dimensions, and hydrogen bonding with water may affect the cutoff pore size.

To achieve the relevant pore sizes for protein separation in the range of a few nanometers, polymer type membranes (dialysis),[6] high temperature silica pore segregation,[5] or several approaches based on self-organized anodic porous alumina (with subsequent diameter reduction using metal[7] or silica filling[8]) have been used.

In principle, a most elegant and effective way for membrane fabrication would be to use directly self-organized porous or tubular oxide structures that can be formed by anodizing suitable metals under optimized conditions.[9−11] However, typical self-organized channels in anodic alumina or titania nanotube membranes are too large (∼20−200 nm in diameter) to be used for most cases of macromolecular separation.

In the present work, we demonstrate that a recently reported new anodization approach[12,13] can be modified to produce titania layers with defined channels that are suitable for size selective protein separation. Free standing, flow-through membrane layers can be produced simply by complete anodic oxidation of thin Ti metal foils. A key advantage of these layers is their photocatalytic activity which can be used for effective declogging of the membranes. Clogging of membranes is a notorious problem occurring in virtually all size separation devices if the pore openings are within the size range of the smallest excluded proteins.

Figure 1a−c show a TiO_2 nanochannel membrane, prepared by complete anodization of a 10 μm thick Ti foil in dehydrated glycerol-K_2HPO_4 solution at 180 °C (see experimental details in Supporting Information (SI)). The final point of the anodization process can easily be determined by recording the current during the process.

Figure 1a shows the foil after the anodization process. It is converted to an oxide layer of approximately 10 μm thickness (i.e., the oxidation efficiency for metal to oxide is in the range of ∼50%). The entire thickness consists of aligned interlinked regular channels with a width in the range of 8−12 nm (Figure S2). The TEM image

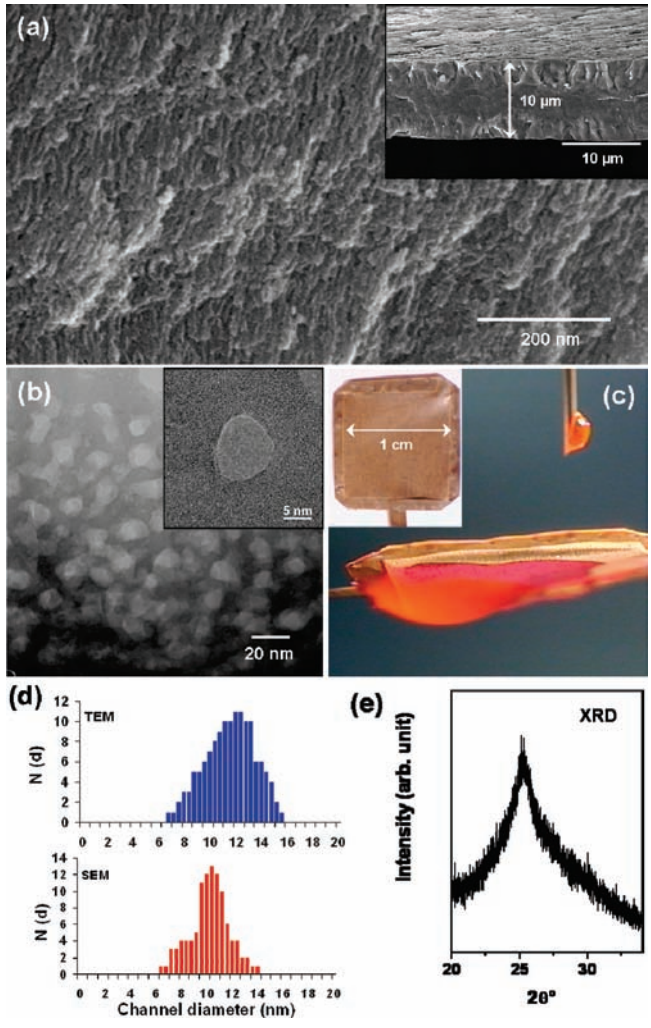

Figure 1. (a) SEM image of the TiO_2 nanochannel membrane formed by complete anodization of a 10 μm thick Ti-foil (inset: cross-sectional view of the full 10 μm thick TiO_2 membrane). (b) TEM plane view image of the nanochannels (inset: HRTEM image showing a single channel). (c) Optical image showing the completely anodized metal anode (∼1 × 1 cm^2). The edges were protected by a silicon polymer; a colored water droplet demonstrates easy permeation of H_2O. (d) Size distribution plot of nanochannel width according to SEM and TEM analyses. (e) XRD pattern of the TiO_2 membrane showing presence of anatase crystallites in oxide.

in Figure 1b confirms the SEM and shows channel openings of ∼8−15 nm in diameter. A statistical evaluation of the size distribution of nanochannels from SEM and TEM images shown in Figure 1d gives an average pore size of 10 ± 2.4 nm for SEM and 11 ± 2.7 nm for TEM with a sharp cutoff of >14−15 nm

[†] Department of Materials Science.
[‡] Department of Physics.

diameters. That is, the anodization process produces a very defined and narrow distribution in pore sizes that is desired for a size separation membrane. The fact that the distribution obtained from TEM shows a slight shift toward higher openings can be ascribed to the TEM sample preparation by ion milling and stereological effects. While the HRTEM in Figure 1b shows mostly amorphous material to be present, the XRD pattern, taken over the entire membrane (Figure 1e), shows that the structure contains also anatase crystallites.[14] Figure 1d demonstrates that comparably large-area membranes (1×1 cm^2) can easily be fabricated and are highly water permeable.

To characterize the permeability of an as-formed sample for macromolecules, three biologically relevant proteins with different Stokes radii[15] were selected [Cytochrome C (12 kDa), 1.63 nm; Bovine Serum Albumin (69 kDa), 3.62 nm; β galactosidase (116 kDa), 6.86 nm]. Based on the channel size distribution (Figure 1d) one may expect an exclusion threshold in the range of a molecular diameter of 3−6 nm. For permeation measurements, membranes were clamped between O-rings of a two-chamber cell (a schematic diagram is given in the SI, Figure S3). The reservoir chamber is filled with a protein solution in phosphate buffered saline (PBS) and the outlet chamber with pure PBS. The content of protein that permeated through the membrane was quantified with a Micro BCA Protein Assay Kit (Pierce) after collecting samples at different time intervals (Figure 2) (see also the SI for details).

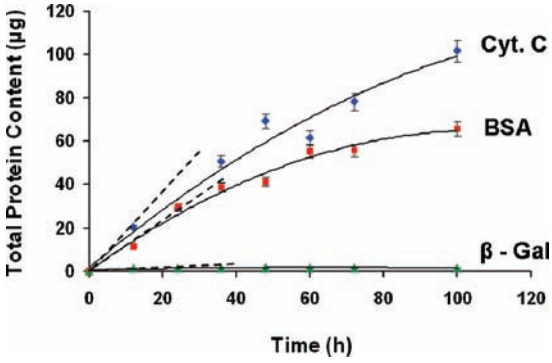

Figure 2. Protein permeation through a 10 μm thick TiO_2 nanochannel membrane (as in Figure 1) vs time for three different size protein molecules: Cyt. C, BSA, and β-Gal. The dotted lines represent the initial slope of the curves.

From Figure 2 it is apparent that the membrane allows Cytochrome C and BSA to pass while, for the largest molecule β-galactosidase, no permeation could be detected even after 3 days of experiments. The permeation flux is clearly faster for small diffusing species (Cyt C, 1.7 μg/h) than the larger one (BSA, 1 μg/h) which simply can be explained by the fact that the diffusion coefficient is inversely proportional to the hydrodynamic radius of the diffusing species.[16] The results presented here are in line with the earlier reports that estimate molecules to be 1/3 the size of the diameter of the channel to be able to pass[4] if hydrated under typical conditions. The results from an experiment where a mixture of all three proteins was used are shown in Figure S4, which demonstrates that, under these conditions, the individual protein fluxes are additive.

A feature frequently observed for molecules in a size range comparable to the pore openings is clogging of the channels as apparent in Figure 2 for BSA by the decrease of the flux with time. Figure 3a shows an extended permeation experiment (160 h) with BSA, where BSA accumulation in the pores steadily reduces the flow until it virtually stops for times longer than 120 h. The inset shows the flux over time, and it is clear that, after ~120 h, a complete blockage of the channels occurs. However, by exploiting the photocatalytic ability of TiO_2,[17,18] the clogged membrane can be treated with brief UV exposure which allows the degradation of the protein molecules and reopening of the pores. This is shown in Figure 3a, where after UV treatment the same membrane can be reused and the initial transfer characteristics are re-established. Clogging and photocatalytic declogging can be confirmed using XPS analysis performed for a membrane after clogging and after UV treatment. Figure 3b shows the elimination of accumulated protein visible in the C1s and N1s peaks after UV exposure. To confirm the specific self-cleaning action of the TiO_2 membrane, the effect of UV irradiation on protein decomposition was investigated on an Al_2O_3 reference surface, where under the same illumination conditions no significant protein degradation could be observed (see SI, Figure S5).

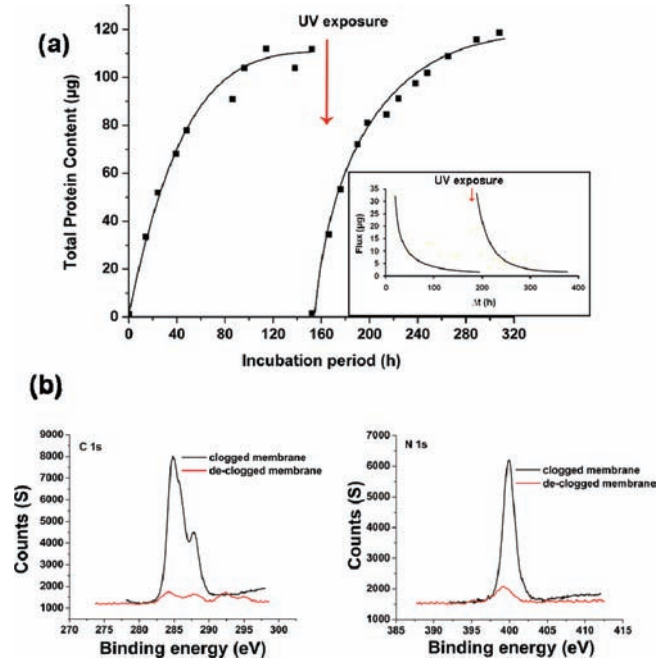

Figure 3. Clogging of membrane by extended permeation and reopening by photocatalytic effect. (a) BSA exposure of the TiO_2 nanochannel membrane resulting in reduced flux and after certain time (120 h) to complete clogging. After 160 h the membrane was UV exposed leading to reopening; *inset*: BSA transport rate. (b) XPS analysis for C1s and N1s peaks of clogged and declogged membrane (after UV exposure).

In conclusion, the present work shows a cheap and effective method to produce free-standing, self-cleaning membranes for size selective macromolecular separation. The nanochannel TiO_2 membrane structure with both sides open can be formed in a single anodization step of a Ti-foil and contains regular channels 8−12 nm in diameter. It should be noted that the size and distribution of the channels formed in our anodic layers are among the smallest and narrowest reported in literature for any self-organized anodic system.[4,5,19,20] In light of considerable work on TiO_2 nanotube membranes[21,22] and the photocatalytic ability of ordered titania structures,[13,23,24] it should be mentioned that the material here after formation already contains anatase crystallites that provide considerable photocatalytic activity; i.e. the material does not need to be annealed which avoids the danger of heat induced crack formation in the membrane production process. Further optimization of the throughput and the declogging efficiency may be achieved by reducing the layer thicknesses combined with patterning of the structures.[22]

Acknowledgment. The authors are thankful to Prof. Dr. Erdmann Spiecker for TEM analysis and acknowledge financial support from the DFG and the DFG Cluster of Excellence (EAM).

Supporting Information Available: Experimental details, XPS analysis, schematic diagram, optical images of the samples. This material is available free of charge via the Internet at http://pubs.acs.org.

References

(1) Bennette, T. P. *Nature* **1967**, 1131.
(2) Martin, C. R. *Science* **1994**, *266*, 1961.
(3) Jirage, K. B.; Hulteen, J. C.; Martin, C. R. *Science* **1997**, *278*, 655–658.
(4) Yu, S.; Lee, S. B.; Kang, M.; Martin, C. R. *Nano Lett.* **2001**, *1*, 495–498.
(5) Striemer, C. C.; Gaborski, T. R.; McGrath, J. L.; Fauchet, P. M. *Nature* **2007**, *445*, 749–753.
(6) Vogelaar, L.; Lammertink, R. G. H.; Barsema, J. N.; Nijdam, W.; Bolhuis-Versteeg, L. A. M.; van Rijn, C. J. M.; Wessling, M. *Small* **2005**, *1*, 645–655.
(7) Müller, F.; Müller, A.-D.; Kröll, M.; Schmid, G. *Appl. Surf. Sci.* **2001**, *171*, 125–129.
(8) Yamaguchi, A.; Uejo, F.; Yoda, T.; Uchida, T.; Tanamura, Y.; Yamashita, T.; Teramae, N. *Nat. Mater.* **2004**, *3*, 337.
(9) Masuda, H.; Fukuda, K. *Science* **1995**, *268*, 1466–1468.
(10) (a) Ghicov, A.; Schmuki, P. *Chem. Commun.* **2009**, 2791–2808. (b) Roy, P.; Berger, S.; Schmuki, P. *Angew. Chem.*, accepted.
(11) Ono, S.; Takeda, K.; Masuko, N. *2nd International symposium on Aluminium Surface Science and Technology, ASST* 2000, UMIST, Manchester, U.K.
(12) Kim, D.; Lee, K.; Roy, P.; Birajdar, B. I.; Spiecker, E.; Schmuki, P. *Angew. Chem., Int. Ed.* **2009**, *48*, 9326.
(13) Lee, K.; Kim, D.; Roy, P.; Paramasivam, I.; Birajdar, B. I.; Spiecker, E.; Schmuki, P. *J. Am. Chem. Soc.* **2010**, *132*, 1478–1479.
(14) Yahalom, J.; Zahavi, J. *Electrochim. Acta* **1970**, *15*, 1429.
(15) Burnett, D.; Wood, S. M.; Bradwell, A. R. *Biochim. Biophys. Acta* **1976**, *427*, 231–237.
(16) Einstein, A. *Ann. Phys.* **1905**, *322*, 549.
(17) Fujishima, A.; Honda, K. *Nature* **1972**, *238*, 37.
(18) Paramasivam, I.; Jha, H.; Schmuki, P. To be submitted.
(19) Ku, J.-R.; Stroeve, P. *Langmuir* **2004**, *20*, 2030–2032.
(20) Vlassiouk, I.; Apel, P. Y.; Dmitriev, S. N.; Healy, K.; Siwy, Z. S. *Proc. Natl. Acad. Sci. U.S.A.* **2009**, *106*, 21039.
(21) Albu, S. P.; Ghicov, A.; Macak, J. M.; Hahn, R.; Schmuki, P. *Nano Lett.* **2007**, *7*, 1286–1289.
(22) Albu, S. P. Ghicov, A.; Berger, S.; Jha, H.; Schmuki, P. Submitted.
(23) Song, Y. Y.; Schmidt-Stein, F.; Bauer, S.; Schmuki, P. *J. Am. Chem. Soc.* **2009**, *131*, 4230.
(24) Shrestha, N. K.; Macak, J. M.; Schmidt-Stein, F.; Hahn, R.; Mierke, C. T.; Fabry, B.; Schmuki, P. *Angew. Chem., Int. Ed.* **2009**, *48*, 969.

JA102712J